

# Proto-OOD: Enhancing OOD Object Detection with Prototype Feature Similarity

Junkun Chen, Jilin Mei, Liang Chen, Fangzhou Zhao, and Yu Hu

Institute of Computing Technology, Chinese Academy of Sciences  
{chenjunkun22s,meijilin,chenliang,zhaofangzhou,huyu}@ict.ac.cn

**Abstract.** The limited training samples for object detectors commonly result in low accuracy out-of-distribution (OOD) object detection. We have observed that feature vectors of the same class tend to cluster tightly in feature space, whereas those of different classes are more scattered. This insight motivates us to leverage feature similarity for OOD detection. Drawing on the concept of prototypes prevalent in few-shot learning, we introduce a novel network architecture, Proto-OOD, designed for this purpose. Proto-OOD enhances prototype representativeness through contrastive loss and identifies OOD data by assessing the similarity between input features and prototypes. It employs a negative embedding generator to create negative embedding, which are then used to train the similarity module. Proto-OOD achieves significantly lower FPR95 in MS-COCO dataset and higher mAP for Pascal VOC dataset, when utilizing Pascal VOC as ID dataset and MS-COCO as OOD dataset. Additionally, we identify limitations in existing evaluation metrics and propose an enhanced evaluation protocol.

**Keywords:** OOD detection · Object detection

## 1 Introduction

Artificial intelligence systems often face a gap between training and real-world application. Training typically involves a subset of class data, while in practice, the model encounters a broader range of data, including unknown classes. This can lead to unreliable predictions for OOD data, potentially causing critical issues, for example, misidentifying OOD data as passable areas in autonomous driving could result in traffic accidents.

Recently, OOD object detection is receiving attention [4, 6, 33]. This task builds upon the accurate object localization of existing detectors by integrating an OOD classifier. The main challenge of this task is to obtain a classifier with high discriminability. SAFE [33] attempts to improve classifier training by generating adversarial samples, but falls short in compensating for the vast discrepancy between adversarial samples and the test set. VOS [6] utilizes a small distance parameter to capture feature outliers for training classifier, but the accuracy of OOD classifier is tied to the optimal distance selection. We believe that the key to addressing these issues is how to extract highly discriminative features for each class from the training data.

Prototype learning has demonstrated strong feature representation capabilities in few-shot tasks [8, 24], inspiring this paper to incorporate the prototype into OOD object detection. As shown in Fig. 1, we notice that feature vectors from the same class cluster closely in feature space, while those from different classes are more distant. This allows us to collect class-specific feature vectors as prototypes. The OOD properties of the input samples are determined by comparing their feature similarity with these prototypes. A high similarity score indicates ID data, while a low similarity score suggests OOD data. Inspired by the Relation Network [27], we utilize a MLP to estimate the similarity scores between the input features and the prototypes.



**Fig. 1:** The feature visualization of Pascal VOC testing set. We employ t-SNE for dimensionality reduction of the feature extractor’s outputs, and each color represents an class.

We introduce Proto-OOD, a novel framework leveraging prototype learning. It collects feature vectors across various classes as prototypes and trains a similarity module to estimate the similarity between input features and these prototypes. Proto-OOD continually updates prototypes during its training stage through weight factors. In order to make prototypes of different classes more representative, contrastive loss is used. Proto-OOD employs a negative embedding generator to create negative embedding, which are then used to train the similarity module. In testing, Proto-OOD performs standard object detection and simultaneously identifies OOD objects. Proto-OOD achieves outstanding performance on the MS-COCO dataset.

Moreover, our experiments reveal that previous methods [4, 6, 33] neglect to filter out inaccurate predictions when assessing metrics on the ID dataset, which leads to poor experimental results. To address this, we refine the current evaluation metrics and re-evaluate the performance of prior methods [4, 6, 33].

The contributions are summarized as follows:

1. To the best of our knowledge, Proto-OOD is pioneering in employing prototype for OOD object detection. Proto-OOD leverages similarity-based detection for OOD objects, reducing the necessity for extensive hyperparameter during testing.

2. Proto-OOD leverages a similarity module to evaluate the similarity between input features and prototypes. It incorporates a negative embedding generator to create negative embeddings, and this strategy negates the requirement for extra OOD datasets during training.

3. Proto-OOD surpasses current methods on MS-COCO [20] and demonstrates significant performance on OpenImages [15]. Furthermore, We improve the rationality of evaluation protocol by filtering out false positives.

## 2 Related Work

### 2.1 OOD Detection for Image Classification

Numerous studies have previously addressed OOD detection for image classification tasks [1, 14, 26, 29, 30, 34, 37]. Vahdat et al. [1] assert the existence of optimal feature layers in the feature space, which can effectively differentiate between ID data and OOD data by leveraging the features in these optimal layers. Meanwhile, Huang et al. [14] propose that the feature distribution of OOD data is concentrated in the feature space. Smith et al. [30] train a RBF network and assess the uncertainty of feature vectors and centroids to distinguish OOD data. Additionally, some approaches aim to introduce noise to the features during model training [22, 28]. Moreover, Mahalanobis distance and enhanced Mahalanobis distance serve as common methods for OOD data detection [17, 23].

A common strategy for OOD detection in image classification involves creating negative examples to train networks. GANs [10] be used to produce low-confidence samples for training, as seen in works by [16, 25, 31]. Du et al. [5] apply stable diffusion to sample outliers in the low-resolution region of the ID data as negative examples. Adversarial examples are also used as OOD data to train classifiers [13, 18].

Several approaches focus on detecting OOD data by examining the distribution of neural network outputs. Yu et al. [36] add a secondary classifier to their model, using the output differences between the two classifiers to spot OOD data. Wang et al. [32] strive to generate a virtual-logit for OOD data. By comparing the output logit with the generated virtual-logit, they can detect OOD data. Dong et al. [3] introduce the neural mean discrepancy method, which identifies OOD data by comparing the neural means of input samples with those of the training data.

Although many papers show significant advancements in OOD detection for image classification, the effectiveness of these methods in the more intricate domain of object detection still needs to be tested.

### 2.2 OOD Detection for Object Detection

There is a scarcity of research on OOD object detection. SIREN [4] introduced a distance-based approach, mapping various classes of features into a hypersphere and utilizing trainable distance parameters to adjust the energy score of

ID data. However, parameters trained on ID data may not be sufficient to distinguish OOD data, as OOD data is not visible during the training phase. VOS [6] samples outliers from the feature space as negative examples to train a classifier. They use a small distance to limit the sampling range, which may result in the error of sampling ID data at the distribution boundary as OOD data. SAFE [33] generates adversarial samples using the fast sign gradient method (FGSM) [11] and employs these adversarial samples as negative examples to train the classifier. SAFE [33] has demonstrated good performance. However, the generated adversarial sample features are too extreme, leading to decreased performance of SAFE when the features of ID and OOD data are similar.

### 2.3 Prototypes for Few-shot Learning

Prototypes have a wide range of applications in few shot learning. Prototype network [24] collects the mean of support set features as the prototypes and computes the distance from the input feature to the prototypes to determine the class. Liu et al. [8] propose a cosine similarity based prototypical network to compute basic prototypes of the novel classes from the few samples. Zhao et al. [38] employ prototypes for few-shot learning on 3D point cloud data. In their method, they use a momentum coefficient to update the prototypes during the training stage, making the prototypes more robust. Gao et al. [9] propose contrastive prototype learning (CPL) for few-shot learning. CPL aims to pull the query samples of the same class closer and those of different classes further away. Allen et al. [2] propose infinite mixture prototypes to adaptively represent data distributions for few-shot learning.

In few-shot learning, prototypes are frequently employed for identifying input feature classes due to their strong categorical representation. This robust attribute can be used for OOD object detection.

## 3 Method

In this section, we present our approach to OOD object detection. The preliminaries and overviews be introduced in section 3.1 and 3.2. In section 3.3, we elucidate the prototype learning and contrastive loss. Following that, in section 3.4, the similarity module and the negative embedding generator are introduced. Finally, in section 3.5, we detail how to train Proto-OOD and how to conduct OOD object detection during the testing stage.

### 3.1 Preliminaries

Let the input image set and label set be  $\mathbf{X}$  and  $\mathbf{Y}$ , respectively.  $Y_{id}=\{1,2,\dots,t\}$  denote ID data class space and  $Y_{ood}$  denote the OOD data class space ( $Y_{id}\cap Y_{ood} = \emptyset$ ). For each  $\mathbf{y} \in \mathbf{Y}$ ,  $\mathbf{y} = \{l, x_{min}, y_{min}, x_{max}, y_{max}\}$  where  $l, (x_{min}, y_{min}, x_{max}, y_{max})$  denote the class label and the coordinate of the object, respectively. During training stage, the ID dataset  $\mathbf{D}^{ID}$  is used to train the model's parameters  $\theta$ . A

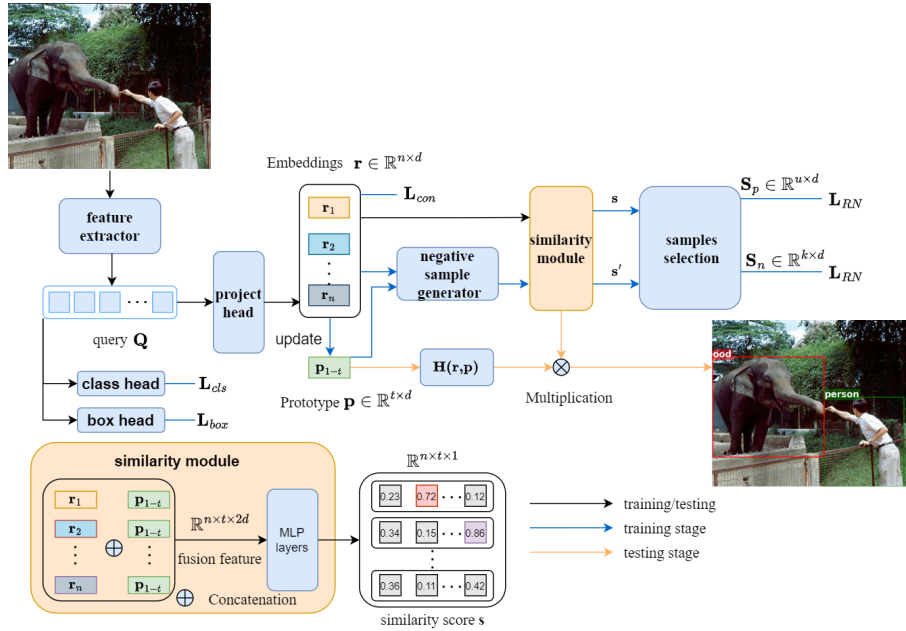


Fig. 2: The framework of Proto-OOD.

subset of the ID dataset  $\mathbf{D}^{ID}$  and the OOD dataset  $\mathbf{D}^{OOD}$  as the test dataset to compute evaluation metrics.

During testing stage, the model not only detects the class and location of the object, but also distinguishes whether the object belongs to ID or OOD data. Given an prediction  $\mathbf{y}^*$  outputted by object detectors and its feature embedding  $\mathbf{r}^*$ , the model estimates the energy  $\mathbf{E}(\mathbf{g}; \mathbf{r}^*, \mathbf{p})$  by the similarity between the  $\mathbf{r}^*$  and the prototypes  $\mathbf{p}$ .  $\mathbf{g} = 1$  indicates that the object belongs to ID data, and  $\mathbf{g} = 0$  indicates that the object belongs to OOD data.

### 3.2 Overviews

We illustrate the framework in **Fig. 2**. We add a similarity module, project head and negative embedding generator to the network to detect OOD data. Given an input image  $\mathbf{x}$ , the feature extractor, utilizing a transformer architecture, processes the image to extract feature query  $\mathbf{Q}$ . The query  $\mathbf{Q}$  is used to predict object class and box by class head and box head.

The project head is a two-layer MLP that maps the query  $\mathbf{Q}$  to a lower-dimensional embedding  $\mathbf{r}$ . Subsequently, the similarity module utilizes the embedding  $\mathbf{r}$  and the prototypes  $\mathbf{p}$  collected during the training stage to predict the similarity score  $\mathbf{s}$ . After combining the similarity score  $\mathbf{s}$  with the cosine similarity between the embedding  $\mathbf{r}$  and the prototypes  $\mathbf{p}$ , it is converted into energy  $\mathbf{E}$ , which is used to determine whether the object belongs to ID or OOD

data. In order to train the similarity module, we select negative scores  $\mathbf{S}_n$  from the result  $\mathbf{s}'$  predicted by the similarity module for negative embeddings  $\mathbf{r}'$ . The details of our algorithm are summarized in Algorithm 1.

### 3.3 Prototype Learning and Contrastive Loss

In the prototype network [24], prototypes are utilized to determine the class of input features. In Proto-OOD, whether the input features belong to OOD data can be determined by the similarity between the input features and the prototypes. Proto-OOD utilizes a project head, a two-layer MLP, to map the query  $\mathbf{Q} \in \mathbb{R}^{n \times h}$  to a lower-dimensional embeddings  $\mathbf{r} \in \mathbb{R}^{n \times d}$  ( $d < h$ ) and collects the prototypes from embeddings  $\mathbf{r}$ . During the early training stage, embeddings  $\mathbf{r}$  may not represent features well. Thus, Proto-OOD collects prototypes after a set number of epochs, using the following method:

$$\mathbf{p}_c = (\alpha \mathbf{p}_c + (1 - \alpha) \mathbf{r}_c) \quad (1)$$

where  $\alpha$  is update factor and  $\mathbf{r}_c$  refers to embeddings from class  $c$ . The original value of  $\mathbf{p}_c$  is  $\mathbf{0}$ .

To enhance the representativeness of prototypes, contrastive loss is added, aiming to enlarge the distances between embeddings  $\mathbf{r}$  of different classes in the feature space. We chose RT-DETR as the object detector. RT-DETR employs the Hungarian algorithm to select the best-matched predictions for calculating the loss. For a batch best-matched predictions, contrastive loss  $\mathbf{L}_{con}$  for embedding  $\mathbf{r}$  is calculated as follow:

$$\mathbf{L}_{con} = \frac{1}{M} \cdot \sum_{i=1}^M f(\bar{r}_i) \quad (2)$$

$$f(z_i) = \begin{cases} -\log \frac{\exp(z_i^\top z_i / \tau)}{\sum_{j=1}^M \exp(z_i^\top z_j / \tau)}, & \|l_i\| = 1 \\ -\log \frac{\sum_{j=1, j \neq i}^M \{y_i == y_j\} \cdot \exp(z_i^\top z_j / \tau)}{\sum_{j=1, j \neq i}^M \exp(z_i^\top z_j / \tau)}, & otherwise \end{cases} \quad (3)$$

where  $\bar{r}_i = z_i = \frac{r_i}{\|r_i\|}$ .  $\tau$  is a scaling factor.  $l_i$  represents the class label of the  $\mathbf{r}_i$ .  $\|l_i\|$  denote the number of objects of class  $l_i$  in a batch of data.  $\|r_i\|$  denote the norm of  $r_i$ .  $M$  is total number of objects in a batch of data.

### 3.4 Similarity Module and Negative Embedding Generator

After collecting representative prototypes, similarity between input features and prototypes can be use to determine whether the object belongs to ID or OOD data. Inspired by the relation network [27], Proto-OOD employs a similarity module to compute the similarity between embeddings  $\mathbf{r}$  and prototypes. The

relation network [27] is proposed for few-shot learning, which utilizes a two-layer MLP to calculate the similarity between the support set features and the query set features, in order to determine the class of the query feature. The embeddings  $\mathbf{r} \in \mathbb{R}^{n \times d}$ , serving as the input of the similarity module, concatenates the prototypes  $\mathbf{p} \in \mathbb{R}^{t \times d}$  to form the fusion features  $\mathbf{f} \in \mathbb{R}^{n \times t \times 2d}$ , where  $t$  is the number of classes. The similarity score  $\mathbf{s}$  predict by a two-layer MLP:

$$\mathbf{s} = \text{Sigmoid}(\sigma(\sigma(\mathbf{f}))) \quad (4)$$

where  $\sigma$  denote  $\text{ReLU}(\text{Linear}(\cdot))$ , and  $\mathbf{s} \in \mathbb{R}^{n \times t \times 1}$ . The similarity score  $\mathbf{s}$  be used to judge OOD data in test-time .

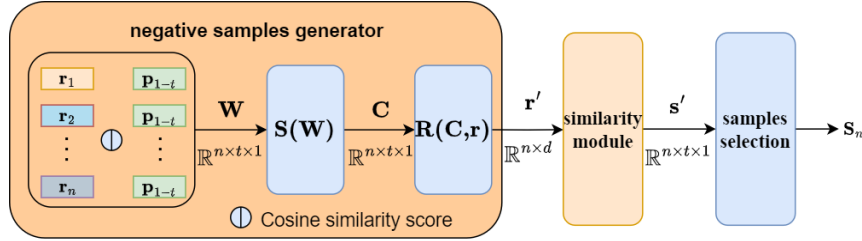


**Fig. 3:** The negative embedding generator generates negative embeddings  $\mathbf{r}'$  after  $\mathbf{R}(\mathbf{C}, \mathbf{r})$ .

We illustrate the negative embedding generator in **Fig. 3**. First, we calculate the cosine similarity  $\mathbf{W} \in \mathbb{R}^{n \times t}$  between the embeddings  $\mathbf{r}$  and prototypes  $\mathbf{p}$ . Then, we use Equation(5) to generate a weight  $\mathbf{C} \in \mathbb{R}^{n \times t}$ , which is used to adjust the ratio of prototypes of different classes. The value in  $\mathbf{C}$  is larger if the prototypes has a lower similarity with embedding  $\mathbf{r}$ . We use a scaling factor  $\mathbf{T}$  to balance the weights of different classes.

$$\mathbf{C} = \mathbf{S}(\mathbf{W}) = \text{Softmax}((\mathbf{1}-\mathbf{W}))/\mathbf{T} \quad (5)$$

We use Equation(6) to generate the negative embeddings  $\mathbf{r}' \in \mathbb{R}^{n \times d}$ .

$$\mathbf{r}' = \mathbf{R}(\mathbf{C}, \mathbf{r}) \quad (6)$$

where  $\mathbf{R}(\mathbf{C}, \mathbf{r})$  process the input as follow :

$$\mathbf{r}'_i = \mathbf{r}_i + \sum_{j=0}^t (\mathbf{C}_{ij} \cdot \mathbf{p}_j) \quad (7)$$

for each  $\mathbf{r}_i \in \mathbf{r}$ , it generates a negative embedding  $\mathbf{r}'_i \in \mathbf{r}'$ . The  $t$  in Equation(7) denotes the number of classes.

---

**Algorithm 1** training and testing

---

**Input:** ID dataset  $\mathbf{D}^{IN}$ , randomly initialize object detector with parameters  $\theta$ , project head with parameters  $\phi$ , similarity module with parameters  $\psi$ , empty prototypes  $\mathbf{O}$ ,  $\lambda$ ,  $\omega$ .

**Output:** object detector, project head, similarity module, prototype feature.

```

1: while training do
2:   if epoch <  $\lambda$  then
3:     Update object detector parameters  $\theta$ , project head parameters  $\phi$  by Equation(10).
4:   else if  $\lambda$  < epoch < ( $\lambda + \omega$ ) then
5:     Update object detector parameters  $\theta$ , project head parameters  $\phi$  by Equation(10). Collect prototypes by Equation (1).
6:   else
7:     Update object detector parameters  $\theta$ , project head parameters  $\phi$ , similarity module parameters  $\psi$  by Equation (11). Collect prototype feature by Equation (1).
8:   end if
9: end while
10: while testing do
11:   Detect objects by object detector with prototypes, and output class score, box location, embedding  $\mathbf{r}$ , similarity score  $\mathbf{s}$ .
12:   Calculate the energy  $\mathbf{E}$  by Equation(12). Output OOD detection results.
13: end while

```

---

### 3.5 Score Selection

To train the similarity module, we need to sample positive and negative similarity scores  $\mathbf{S}_p$  and  $\mathbf{S}_n$ . We choose the Hungarian algorithm to select positive similarity score. The best-matched results of the Hungarian algorithm are sampled as positive scores  $\mathbf{S}_p$  to train the similarity module. These positive scores  $\mathbf{S}_p$  ensure that the similarity module outputs a high similarity score  $\mathbf{s}$  for ID data. Additionally, we need to sample negative similarity scores  $\mathbf{S}_n$ . The negative similarity scores  $\mathbf{S}_n$  sampled from  $\mathbf{s}'$  which generated from negative embeddings  $\mathbf{r}'$  using a similarity module.

Then, We compute the similarity scores  $\mathbf{s}'$  of the embeddings  $\mathbf{r}'$ . We sample negative similarity scores  $\mathbf{S}_n$  from  $\mathbf{s}'$  that are less than a threshold to train similarity module. During the loss calculation stage, We choose several objects that have the lowest IOU with the ground true box and use their similarity score as negative similarity score for training similarity module.

We use the focal loss [19] train the two-layer MLP in similarity module:

$$\mathbf{L}_{RN} = focal\_loss(S, l_{rn}) \tag{8}$$

$$l_{rn} = \begin{cases} l, & S \in S_p \\ 0, & S \in S_n \end{cases} \tag{9}$$

where  $S$  denote similarity scores ,  $l_{rn}$  is the label of the  $S$ .



### 3.6 Training and Testing

Training and testing procedures are represented in Algorithm 1. During training stage, because the representation of embeddings  $\mathbf{r}$  are poor in the early stages of training, we set a hyperparameter  $\lambda$  to determine when to start collecting prototypes. Specifically, when the training epoch is greater than  $\lambda$ , Proto-OOD start to collect prototypes. We first train the object detector with parameters  $\theta$  and the project head with parameters  $\phi$  in *stage1* (line 1 to line 5 in Algorithm 1). The loss function is as follow:

$$\mathbf{L}_{stage1} = \mathbf{L}_{cls} + \mathbf{L}_{box} + \mathbf{L}_{con} \quad (10)$$

When epoch is greater than  $\lambda$ , we begin to collect prototypes. After  $\omega$  epochs, we have collected some robust prototypes, and then, we begin to train the similarity module. The loss in *stage2* (line 6 to line 7 Algorithm 1) as follow:

$$\mathbf{L}_{stage2} = \mathbf{L}_{cls} + \mathbf{L}_{box} + \mathbf{L}_{con} + \mathbf{L}_{RN} \quad (11)$$

where the  $\mathbf{L}_{cls}$  is *focal\_loss* [19], and  $\mathbf{L}_{box}$  is L1 loss.

After training the entire network, we can obtain an object detector with OOD detection functionality.

During testing stage, the object detector outputs not only the class score and box position, but also the object feature embeddings  $\mathbf{r}$  and similarity score  $\mathbf{s}$ .

Given a object embedding  $\mathbf{r}^*$ , the energy  $\mathbf{E}(\mathbf{g}; \mathbf{r}^*, \mathbf{p})$  generated by embedding  $\mathbf{r}^*$  and prototypes  $\mathbf{p}$  is used to determine whether the object belongs to the ID data. The energy  $\mathbf{E}(\mathbf{g}; \mathbf{r}^*, \mathbf{p})$  is calculated as follow:

$$\mathbf{E}(\mathbf{g}; \mathbf{r}^*, \mathbf{p}) = \mathbf{H}(\mathbf{r}^*, \mathbf{p}) \cdot \mathbf{s}^* = \exp(\text{Cosine\_similarity}(\mathbf{r}^*, \mathbf{p})) \cdot \mathbf{s}^* \quad (12)$$

where  $\mathbf{p}$  denote prototypes.  $\mathbf{s}^*$  represents the similarity score output by the similarity module. We set a threshold  $\gamma$  for the energy  $\mathbf{E}(\mathbf{g}; \mathbf{r}^*, \mathbf{p})$  to distinguish between ID and OOD objects:

$$\mathbf{g}(\mathbf{r}^*, \mathbf{p}) = \begin{cases} 1, & \mathbf{E}(\mathbf{g}; \mathbf{r}^*, \mathbf{p}) \geq \gamma \\ 0, & \mathbf{E}(\mathbf{g}; \mathbf{r}^*, \mathbf{p}) < \gamma \end{cases} \quad (13)$$

if  $\mathbf{g}(\mathbf{r}^*, \mathbf{p})$  equals 1, the object is considered as ID data. If  $\mathbf{g}(\mathbf{r}^*, \mathbf{p})$  equals 0, the object is considered as OOD data.

## 4 Experiments

In Section 4.1, we present the experimental setup. In Section 4.2, we introduce the evaluation metrics and come up with an improved evaluation protocol. Experimental results also displayed in this section.

#### 4.1 Experimental Setting

**Datasets.** Same as SIREN [4], we use the PASCAL-VOC [7] and Berkley DeepDrive-100K [35] (BDD100K) datasets as our ID datasets for training and evaluation. The subset of the MS-COCO [20] and OpenImages [15] are used as OOD dataset to evaluation.

**Implementation Details.** The RT-DETR [21], with ResNet50 [12] as its backbone, is utilized as an object detector. We set the scaling factor  $\tau=0.2$  in Equation(3), and the scaling factor  $\mathbf{T}=2$  in Equation(5). For Pascal VOC [7] dataset, the  $\lambda = 40$  and the  $\omega = 5$ , which means that the prototypes collected after 40 epoch, and the similarity module trained after 45 epoch. For BDD100K [35], the  $\lambda = 25$  and the  $\omega = 5$ . We discover that the model predicts many inaccurate results when testing ID data, including boxes containing only background or with a small IOU with ground true box. Consequently, for OOD metrics evaluation, we selectively choose K objects with the highest scores from the ID dataset, where K corresponds to the number of labeled objects in an image. When evaluation OOD detection metrics, to prevent a single object from participating repeatedly in the computation, Non-maximum suppression(NMS) is utilized in the post-processing stage.

#### 4.2 Evaluation Metrics and Results

**Evaluation Protocol.** We utilize the evaluation protocol as **protocol<sub>A</sub>** defined by SIREN [4] to evaluation Proto-OOD. we report the metric mAP for ID dataset. For OOD dataset, we report the false positive rate of samples when the true positive rate of ID objects is at 95% (**FPR95**) and the area under the receiver operating characteristic curve (**AUROC**). A lower FPR95 indicates superior model performance, while a higher AUROC signifies better model performance. Additionally, we note that previous methods [4, 6, 33] overlook the filter out inaccurate predictions when calculating metrics. This may lead to inaccuracies in their OOD evaluation metrics. Specifically, the formula for the false positive rate (FPR) is as follows:

$$FPR = \frac{FP}{FP + TN} \quad (14)$$

where  $FP$  represents the misclassification of negative samples as positive samples and  $TN$  indicates that the negative sample is correctly predicted to be negative. Previous methods [4, 6, 33] don't filtering out inaccurate predictions that led to  $FP$  in Equation(14) being too large when calculating  $FPR$ .

Hence, we propose a new evaluation protocol as **protocol<sub>B</sub>**. To avoid these inaccurate predictions leading to an increase in  $FP$ , only the K objects with the highest score are selected when calculating the OOD detection metrics for the ID dataset, where K is equal to the number of annotated objects in the image.

**Results and Analysis.** The performance of Proto-OOD under **protocol<sub>A</sub>** compared with other methods is shown in the **Table 1**. It is not surprising that Proto-OOD achieves the best FRP95 and AUROC on MS-COCO when using

**Table 1:** Detection results comparing our method to current OOD object detection method.  $\uparrow$  indicates larger AUROC are better.  $\downarrow$  indicates smaller FPR95 are better. Bold numbers indicate the best performance.

ID dataset	method	OOD:MS-COCO/OpenImages		mAP
		FPR95 $\downarrow$	AUROC $\uparrow$	
Pascal VOC	SIREN-VMF [4](2022)	75.49 $\pm$ 0.8/78.36 $\pm$ 1.0	76.10 $\pm$ 0.1/71.05 $\pm$ 0.1	60.8 $\pm$ 0.1
	SIREN-KNN [4](2022)	64.77 $\pm$ 0.2/65.99 $\pm$ 0.5	78.23 $\pm$ 0.2/74.93 $\pm$ 0.1	60.8 $\pm$ 0.1
	VOS-RegNetX4.0 [6](2022)	47.77 $\pm$ 1.1/48.33 $\pm$ 1.6	89.00 $\pm$ 0.4/87.59 $\pm$ 0.2	51.6 $\pm$ 0.1
	VOS-ResNet50 [6](2022)	47.53 $\pm$ 2.9/51.33 $\pm$ 1.6	88.70 $\pm$ 1.2/85.23 $\pm$ 0.6	48.9 $\pm$ 0.2
	SAFE-ResNet50 [33](2023)	47.40 $\pm$ 3.8/20.06 $\pm$ 2.3	80.30 $\pm$ 2.4/92.28 $\pm$ 1.0	/
	SAFE-RegNetX4.0 [33](2023)	36.32 $\pm$ 1.1/17.69 $\pm$ 1.0	87.03 $\pm$ 0.5/94.30 $\pm$ 0.2	/
	Proto-OOD(ours)	<b>20.98<math>\pm</math>1.5</b> /28.25 $\pm$ 3.7	95.23 $\pm$ 0.2/91.73 $\pm$ 1.0	64.32
BDD100k	SIREN-VMF [4](2022)	67.54 $\pm$ 1.3/66.31 $\pm$ 0.9	80.06 $\pm$ 0.5/79.77 $\pm$ 1.2	31.3 $\pm$ 0.0
	SIREN-KNN [4](2022)	53.97 $\pm$ 0.7/47.28 $\pm$ 0.3	86.56 $\pm$ 0.1/89.00 $\pm$ 0.4	31.3 $\pm$ 0.0
	VOS-RegNetX4.0 [6](2022)	36.61 $\pm$ 0.9/27.24 $\pm$ 1.3	89.08 $\pm$ 0.6/92.13 $\pm$ 0.5	32.5 $\pm$ 0.1
	VOS-ResNet50 [6](2022)	44.27 $\pm$ 2.0/35.54 $\pm$ 1.7	86.87 $\pm$ 2.1/88.52 $\pm$ 1.3	31.3 $\pm$ 0.0
	SAFE-ResNet50 [33](2023)	32.56 $\pm$ 0.8/16.04 $\pm$ 0.5	88.96 $\pm$ 0.6/94.64 $\pm$ 0.3	/
	SAFE-RegNetX4.0 [33](2023)	21.69 $\pm$ 0.5/13.98 $\pm$ 0.3	93.91 $\pm$ 0.1/95.57 $\pm$ 0.1	/
	Proto-OOD(ours)	7.85 $\pm$ 0.92/9.60 $\pm$ 1.6	98.40 $\pm$ 0.2/98.14 $\pm$ 0.3	31.7 $\pm$ 0.1

Pascal VOC as the ID dataset, as we filtering out inaccurate predictions in the ID dataset. Furthermore, due to the contrastive loss, Proto-OOD also significantly outperforms other methods in mAP. What interests us is that when utilizing BDD100K as the ID dataset, Proto-OOD achieves the best FPR and AUROC on both MS-COCO and OpenImages. We analyze the following three possible reasons:

(1) BDD100K has a large number of images in the training set. Meanwhile, BDD100K is a data set of road scenes, which enables Proto-OOD to collect very representative prototypes during training stage. Therefore, Proto-OOD is able to achieve excellent performance on MS-COCO and OpenImages, as these datasets exhibit substantial differences from BDD100K.

(2) BDD100K has far more test images than MS-COCO and Openimages in test set. Therefore, BDD100K have a greater impact on evaluation metrics.

(3) The feature extractor, RT-DETR [21], does not have a structure similar to RPN in Faster-RCNN to suppress the background region, so when tested with MS-COCO and Openimages dataset, RT-DETR becomes extremely sensitive, resulting in a large number of low-scoring OOD predictions, which enlarge the value of  $TN$  in Equation(14).

These reasons are also factors that we considered when establishing the **protocol<sub>B</sub>**. We evaluate all the methods [4, 6, 33] in **protocol<sub>B</sub>** and results are showed in **Table 2**. The results indicate that previous methods [4, 6, 33] improve performance by filtering out inaccurate output when testing ID data. The FPR for SIREN [4] decreased by more than 30%. The performance of VOS [6] also improves significantly. SAFE continues to get the best performance on Openimages.

**Table 2:** The performance of under the **protocol<sub>B</sub>**

ID dataset	method	OOD:MS-COCO/OpenImages		mAP
		FPR95↓	AUROC↑	
Pascal VOC	SIREN-VMF	75.49/78.36	76.10/71.05	60.8±0.1
	SIREN-VMF*	44.60/54.14	90.95/85.39	60.8±0.1
	VOS-ResNet50	47.53/51.33	88.70/85.23	51.6±0.1
	VOS-ResNet50*	35.64/44.16	90.06/88.59	48.9±0.2
	SAFE-ResNet50	47.40/20.06	80.30/92.28	/
	SAFE-ResNet50*	44.74/22.97	82.37/92.61	/
	Proto-OOD* (ours)	20.98/28.25	95.23/91.73	64.32

\* represents results tested under the **protocol<sub>B</sub>**

## 5 Conclusion

We propose Proto-OOD network architecture for OOD object detection. Proto-OOD is a structure that uses prototypes for OOD object detection for the first time. Proto-OOD distinguishes whether the input features belong to ID or OOD data use similarity. Proto-OOD provides a new way for OOD object detection.

Proto-OOD gradually collects prototypes of ID data during the training stage, and samples negative samples with low similarity to the prototype in the feature space to train a similarity module, so that the similarity module can be used as an effective similarity predictor. Proto-OOD shows good performance for OOD object detection.

Furthermore, We elucidate the limitations of current detection metrics, and come up with a more reasonable evaluation protocol. Later, we will endeavor to explore benchmarks for OOD object detection.

## References

1. Abdelzad, V., Czarnecki, K., Salay, R., Denouden, T., Vernekar, S., Phan, B.: Detecting out-of-distribution inputs in deep neural networks using an early-layer output. arXiv preprint arXiv:1910.10307 (2019) **3**
2. Allen, K., Shelhamer, E., Shin, H., Tenenbaum, J.: Infinite mixture prototypes for few-shot learning. In: Chaudhuri, K., Salakhutdinov, R. (eds.) Proceedings of the 36th International Conference on Machine Learning. Proceedings of Machine Learning Research, vol. 97, pp. 232–241. PMLR (09–15 Jun 2019), <https://proceedings.mlr.press/v97/allen19b.html> **4**
3. Dong, X., Guo, J., Li, A., Ting, W.T.M., Liu, C., Kung, H.: Neural mean discrepancy for efficient out-of-distribution detection. 2022 iee. In: CVF Conference on Computer Vision and Pattern Recognition (CVPR). pp. 19195–19205 (2021) **3**
4. Du, X., Gozum, G., Ming, Y., Li, Y.: Siren: Shaping representations for detecting out-of-distribution objects. In: Advances in Neural Information Processing Systems (2022) **1, 2, 3, 10, 11**

5. Du, X., Sun, Y., Zhu, J., Li, Y.: Dream the impossible: Outlier imagination with diffusion models. *Advances in Neural Information Processing Systems* **36** (2024) [3](#)
6. Du, X., Wang, Z., Cai, M., Li, Y.: Vos: Learning what you don't know by virtual outlier synthesis. *Proceedings of the International Conference on Learning Representations* (2022) [1](#), [2](#), [4](#), [10](#), [11](#)
7. Everingham, M., Eslami, S.M.A., Van Gool, L., Williams, C.K.I., Winn, J., Zisserman, A.: The pascal visual object classes challenge: A retrospective. *International Journal of Computer Vision* **111**(1), 98–136 (Jan 2015) [10](#)
8. Fu, Z., Kong, Y., Zheng, Y., Ye, H., Hu, W., Yang, J., He, L.: Cascaded detail-preserving networks for super-resolution of document images. *CoRR* [abs/1911.10714](#) (2019), <http://arxiv.org/abs/1911.10714> [2](#), [4](#)
9. Gao, Y., Fei, N., Liu, G., Lu, Z., Xiang, T.: Contrastive prototype learning with augmented embeddings for few-shot learning. In: de Campos, C., Maathuis, M.H. (eds.) *Proceedings of the Thirty-Seventh Conference on Uncertainty in Artificial Intelligence. Proceedings of Machine Learning Research*, vol. 161, pp. 140–150. PMLR (27–30 Jul 2021), <https://proceedings.mlr.press/v161/gao21a.html> [4](#)
10. Goodfellow, I., Pouget-Abadie, J., Mirza, M., Xu, B., Warde-Farley, D., Ozair, S., Courville, A., Bengio, Y.: Generative adversarial networks. *Communications of the ACM* **63**(11), 139–144 (2020) [3](#)
11. Goodfellow, I.J., Shlens, J., Szegedy, C.: Explaining and harnessing adversarial examples. *arXiv preprint arXiv:1412.6572* (2014) [4](#)
12. He, K., Zhang, X., Ren, S., Sun, J.: Deep residual learning for image recognition. In: *Proceedings of the IEEE conference on computer vision and pattern recognition*. pp. 770–778 (2016) [10](#)
13. Hsu, Y.C., Shen, Y., Jin, H., Kira, Z.: Generalized odin: Detecting out-of-distribution image without learning from out-of-distribution data. In: *Proceedings of the IEEE/CVF Conference on Computer Vision and Pattern Recognition*. pp. 10951–10960 (2020) [3](#)
14. Huang, H., Li, Z., Wang, L., Chen, S., Dong, B., Zhou, X.: Feature space singularity for out-of-distribution detection. *arXiv preprint arXiv:2011.14654* (2020) [3](#)
15. Krasin, I., Duerig, T., Alldrin, N., Ferrari, V., Abu-El-Haija, S., Kuznetsova, A., Rom, H., Uijlings, J., Popov, S., Veit, A., Belongie, S., Gomes, V., Gupta, A., Sun, C., Chechik, G., Cai, D., Feng, Z., Narayanan, D., Murphy, K.: Openimages: A public dataset for large-scale multi-label and multi-class classification. Dataset available from <https://github.com/openimages> (2017) [3](#), [10](#)
16. Lee, K., Lee, H., Lee, K., Shin, J.: Training confidence-calibrated classifiers for detecting out-of-distribution samples. *arXiv preprint arXiv:1711.09325* (2017) [3](#)
17. Lee, K., Lee, K., Lee, H., Shin, J.: A simple unified framework for detecting out-of-distribution samples and adversarial attacks. *Advances in neural information processing systems* **31** (2018) [3](#)
18. Liang, S., Li, Y., Srikant, R.: Enhancing the reliability of out-of-distribution image detection in neural networks. *arXiv preprint arXiv:1706.02690* (2017) [3](#)
19. Lin, T.Y., Goyal, P., Girshick, R., He, K., Dollár, P.: Focal loss for dense object detection. In: *Proceedings of the IEEE international conference on computer vision*. pp. 2980–2988 (2017) [8](#), [9](#)
20. Lin, T., Maire, M., Belongie, S.J., Bourdev, L.D., Girshick, R.B., Hays, J., Perona, P., Ramanan, D., Dollár, P., Zitnick, C.L.: Microsoft COCO: common objects in context. *CoRR* [abs/1405.0312](#) (2014), <http://arxiv.org/abs/1405.0312> [3](#), [10](#)
21. Lv, W., Xu, S., Zhao, Y., Wang, G., Wei, J., Cui, C., Du, Y., Dang, Q., Liu, Y.: Detsr beat yolos on real-time object detection. *arXiv preprint arXiv:2304.08069* (2023) [10](#), [11](#)

22. Mahmood, A., Oliva, J., Styner, M.: Multiscale score matching for out-of-distribution detection. arXiv preprint arXiv:2010.13132 (2020) [3](#)
23. Ren, J., Fort, S., Liu, J., Roy, A.G., Padhy, S., Lakshminarayanan, B.: A simple fix to mahalanobis distance for improving near-ood detection. arXiv preprint arXiv:2106.09022 (2021) [3](#)
24. Snell, J., Swersky, K., Zemel, R.: Prototypical networks for few-shot learning. Advances in neural information processing systems **30** (2017) [2](#), [4](#), [6](#)
25. Sricharan, K., Srivastava, A.: Building robust classifiers through generation of confident out of distribution examples. arXiv preprint arXiv:1812.00239 (2018) [3](#)
26. Sun, Y., Ming, Y., Zhu, X., Li, Y.: Out-of-distribution detection with deep nearest neighbors. In: International Conference on Machine Learning. pp. 20827–20840. PMLR (2022) [3](#)
27. Sung, F., Yang, Y., Zhang, L., Xiang, T., Torr, P.H., Hospedales, T.M.: Learning to compare: Relation network for few-shot learning. In: Proceedings of the IEEE conference on computer vision and pattern recognition. pp. 1199–1208 (2018) [2](#), [6](#), [7](#)
28. Tack, J., Mo, S., Jeong, J., Shin, J.: Csi: Novelty detection via contrastive learning on distributionally shifted instances. Advances in neural information processing systems **33**, 11839–11852 (2020) [3](#)
29. Tao, L., Du, X., Zhu, J., Li, Y.: Non-parametric outlier synthesis. In: The Eleventh International Conference on Learning Representations (2023), <https://openreview.net/forum?id=JHk1pEZqduQ> [3](#)
30. Van Amersfoort, J., Smith, L., Teh, Y.W., Gal, Y.: Uncertainty estimation using a single deep deterministic neural network. In: International conference on machine learning. pp. 9690–9700. PMLR (2020) [3](#)
31. Vernekar, S., Gaurav, A., Abdelzad, V., Denouden, T., Salay, R., Czarnecki, K.: Out-of-distribution detection in classifiers via generation. arXiv preprint arXiv:1910.04241 (2019) [3](#)
32. Wang, H., Li, Z., Feng, L., Zhang, W.: Vim: Out-of-distribution with virtual-logit matching. In: Proceedings of the IEEE/CVF conference on computer vision and pattern recognition. pp. 4921–4930 (2022) [3](#)
33. Wilson, S., Fischer, T., Dayoub, F., Miller, D., Sünderhauf, N.: Safe: Sensitivity-aware features for out-of-distribution object detection. In: Proceedings of the IEEE/CVF International Conference on Computer Vision (ICCV). pp. 23565–23576 (October 2023) [1](#), [2](#), [4](#), [10](#), [11](#)
34. Wilson, S., Fischer, T., Sünderhauf, N., Dayoub, F.: Hyperdimensional feature fusion for out-of-distribution detection. In: Proceedings of the IEEE/CVF Winter Conference on Applications of Computer Vision. pp. 2644–2654 (2023) [3](#)
35. Xu, H., Gao, Y., Yu, F., Darrell, T.: End-to-end learning of driving models from large-scale video datasets. CoRR **abs/1612.01079** (2016), <http://arxiv.org/abs/1612.01079> [10](#)
36. Yu, Q., Aizawa, K.: Unsupervised out-of-distribution detection by maximum classifier discrepancy. In: Proceedings of the IEEE/CVF international conference on computer vision. pp. 9518–9526 (2019) [3](#)
37. Zaeemzadeh, A., Bisagno, N., Sambugaro, Z., Conci, N., Rahnavard, N., Shah, M.: Out-of-distribution detection using union of 1-dimensional subspaces. In: Proceedings of the IEEE/CVF conference on Computer Vision and Pattern Recognition. pp. 9452–9461 (2021) [3](#)
38. Zhao, S., Qi, X.: Prototypical votenet for few-shot 3d point cloud object detection. In: Advances in Neural Information Processing Systems (2022) [4](#)